# Numerical solutions to dilaton gravity models and the semiclassical singularity

J. D. Hayward*

*Department of Applied Mathematics and Theoretical Physics, University of Cambridge, Silver Street, Cambridge CB3 9EW, United Kingdom*

(Received 16 May 1995; revised manuscript received 18 July 1995)

A general homogeneous two-dimensional dilaton gravity model considered recently by Lemos and Sà is given quantum matter Polyakov corrections and is solved numerically for several static, equilibrium scenarios. Classically the dilaton field ranges the whole real line, whereas in the semiclassical theory, with the usual definition, it is always below a certain critical value at which a singularity appears. We give solutions for both sub- and supercritical dilaton fields. The pasting together of the spacetime on both sides of a singularity in semiclassical planar general relativity is discussed.

PACS number(s): 04.70.Dy, 04.60.Kz

## I. INTRODUCTION

The machinations of black holes have been studied extensively in recent years using two-dimensional models [1–3].

In [4, 5], the original Callan-Giddings-Harvey-Strominger (CGHS) model was solved numerically for explicitly static equilibrium scenarios. The CGHS Lagrangian is a dilaton gravity model which is made up of a classical part, which comes directly from low energy string theory in two dimensions, and a quantum correction described by Polyakov in [6] which takes into account the one-loop effects of the matter fields. The number of these fields can be proliferated so that the effect of other quantum corrections is small compared to that of the matter. In another paper, by Lemos and Sà [7], the classical Lagrangian considered is more general than that of the CGHS model. A variable multiplicative parameter is included in the kinetic dilaton term. By choosing certain values for this parameter, a set of classical models which includes low energy string theory in two dimensions, Jackiw-Teitelboim theory, and planar general relativity is obtained.

In this paper, the idea is to combine and extend the work of [7] and [4, 5]. The more general classical core Lagrangian of [7] will be combined with the Polyakov quantum matter correction, and a set of static numerical solutions to various models with and without the correction is displayed. The static black holes in equilibrium with Hawking radiation can be studied numerically. One motivation for studying such solutions is to understand the "semiclassical" singularity which was discovered shortly after the appearance of the original CGHS paper [8, 9]. Birnir *et al.* noted that this singularity occurred at a finite dilaton value, and that the metric was actually finite there, unlike the classical case. We investigate this further here. The static solutions might be a candidate final state of black hole evaporation, i.e., as massive remnants. This was rejected in [4] since the Arnowitt-Deser-Misner (ADM) mass for these solutions is divergent because there is nonzero radiation density out to infinity. Here we shall find the expression for the ADM mass in that case and show that it is indeed infinite. For equilibrium in two dimensions, this divergence is actually necessary, but we shall see that the solutions are nevertheless interesting.

In the following section, a general two-dimensional homogeneous dilaton gravity model is introduced, whose field equations for static solutions are written down. The initial conditions for regular-horizon spacetimes are then given.

In Sec. III, a general introduction to the results is given. Static regular-horizon solutions in which the dilaton is initially and remains sub- or supercritical are then found for a range of classical cores with and without quantum corrections. The solutions being static and numerical, it is difficult to be precise about global structure away from the singularities at infinity, though one can give some details about the singularity itself and the horizon. We restrict a fuller description and interpretation to the case whose classical core is that of planar general relativity.

In Sec. IV are the conclusion and discussion.

## II. GENERAL HOMOGENEOUS TWO-DIMENSIONAL MODEL

### A. Introduction

A general homogeneous Lagrangian with semiclassical minimal scalars is of the form

$$I=\frac{1}{2\pi}\int d^2x\sqrt{\pm g}\Big[R\tilde{\chi}(\Phi)+4\omega e^{-2\phi}\nabla\phi^2+V(\Phi) -\frac{\kappa}{4}\nabla Z^2-\frac{1}{2}\sum_{i=1}^{N}(\nabla f_i)^2\Big]-\frac{1}{\pi}\int d\Sigma\sqrt{\pm h}K\tilde{\chi}, \tag{1}$$

where $\tilde{\chi}=\frac{\kappa}{2}Z+\Phi$, and $\Phi$ is a function of the dilaton field $\phi$ and any other fields that are required.

*Electronic address: J.D.Hayward@damtp.cam.ac.uk

 

The terms involving $Z$ in the volume term of this action have replaced the usual Polyakov term [6] $\frac{\kappa}{4}R(x)\int d^2x'\sqrt{-g(x')}G(x,x')R(x')$ which comes from the matter contribution to the associated path integral. $G(x,x')$ is the scalar Green's function. The trace anomaly of the $Z$ scalar field is that of the $N$ minimal scalars.

One could choose the function of the dilaton field so as to make the theory have vanishing central charge [10], but for simplicity models for which $V(\Phi)=4\lambda^2$ will be restricted here. The function $\tilde{\chi}$ takes into account both the classical coupling of the dilaton to gravity and any one-loop terms which come from quantizing additional fields. The classical part will be taken to be $e^{-2\phi}$ and the one-loop corrections to be those of the CGHS model, so that $\tilde{\chi}=e^{-2\phi}-\frac{\kappa}{2}(\epsilon\phi-Z)$, where[1] $\epsilon=0$. The CGHS model is regained when $\omega=1$.

If one tries to work in the two-dimensional analogy of the "Eddington-Finkelstein" gauge [11], the action and field equations are still complicated although the work on entropy which depends on the position of the horizon might be simplified. However, for static solutions one should use the conformal gauge where the line element is

$$dl^2=-e^{2\rho}dx^+dx^-. \tag{2}$$

The field equations then imply that $Z=2\rho$, up to a solution of the wave equation.

The action (1) now becomes

$$I=-\frac{1}{\pi}\int d^2x\sqrt{g}\Big[e^{-2\phi}(2\partial_-\partial_+\rho-4\omega\partial_-\phi\partial_+\phi+\lambda^2e^{2\rho}) +\frac{1}{2}\partial_+f_i\partial_-f_i-\kappa(\partial_-\rho\partial_+\rho+\epsilon\phi\partial_-\partial_+\rho)\Big], \tag{3}$$

where the term involving $f_i$ is summed as in (1). The surface term is omitted from now on.

### B. Field equations

The following applies to static solutions which are functions of the static variable $s=-x^+x^-$ only. Terms in $f_i$ have been set to zero. Denoting $'=\frac{d}{ds}$, the field equations become

$$Q(\phi)\left[\phi''+\frac{1}{s}\phi'\right]=2\phi'^2[P(\epsilon,\phi)-\tfrac{1}{2}\omega\kappa e^{2\phi}] -\frac{\lambda^2}{2s}e^{2\rho}[P(\epsilon,\phi)-\tfrac{1}{2}\kappa e^{2\phi}], \tag{4}$$

$$Q(\phi)\left[\rho''+\frac{1}{s}\rho'\right]=2\omega\phi'^2[2-P(\epsilon,\phi)] -\frac{\lambda^2}{2s}e^{2\rho}[2\omega-P(\epsilon,\phi)], \tag{5}$$

where $P(\epsilon,\phi)=1+\frac{\epsilon\kappa}{4}e^{2\phi}$ and $Q(\phi)=P(\epsilon,\phi)^2-\omega\kappa e^{2\phi}$.

The constraint equations are

$$P(\epsilon,\phi)(\phi''-2\rho'\phi')+2(\omega-1)\phi'^2 +\frac{1}{2}\kappa e^{2\phi}\left(\rho'^2-\rho''+\frac{t}{s^2}\right)=0, \tag{6}$$

where $t$ is given by the boundary conditions required. These equations which will reduce in the case of $\omega=1$ to either the CGHS ($\epsilon=0$) or RST ($\epsilon=1$) model.

### C. Initial conditions

One can solve the dynamical equations numerically for $\rho$, $\phi$, and their derivatives, by rewriting them as a coupled set of four first order differential equations. The boundary conditions chosen are such that the origin in $s$ is regular. This requires that

$$s\rho''(0)=s\phi''(0)=0, \tag{7}$$

$$t=0, \tag{8}$$

A shift in $\rho$ allows one to remove $\lambda$ from the equations. $\phi$ can also be redefined so that the equations are independent of $\kappa$. One then finds that the derivatives at the origin should be

$$\rho'(0)=\frac{-\frac{1}{2}e^{2\rho_0}[P(\phi_0)-2\omega]}{Q(\phi_0)}, \tag{9}$$

$$\phi'(0)=\frac{-\frac{1}{2}e^{2\rho_0}[P(\phi_0)-\frac{1}{2}e^{2\phi_0}]}{Q(\phi_0)}. \tag{10}$$

These equations reduce to those of [2] in the case $\omega=1,\epsilon=0$.

Varying the initial value of $\rho$ simply scales the equations. The initial value of $\phi$ at the origin is related to the "size" of the black hole. That is, moving towards the critical value initially reduces the coordinate distance to the singularity from the horizon.

### D. Choice of $\omega$ parameter

In order to choose the smallest set of values of $\omega$ each of which produce a different behavior, one can consider expression (21) for the curvature, $R=-8e^{-2\rho}(\frac{d}{ds}+s\frac{d^2}{ds^2})\rho$, the field equations (4),(5), and the values of $\omega$ and $\phi_0$ which change the sign of the initial values of $\frac{d\rho}{ds}$ and $\frac{d\phi}{ds}$. The critical value[2] of $\phi$ is given by

$$\phi_{\rm cr}=-\frac{1}{2}\ln\omega. \tag{11}$$

Singularities will therefore occur at increasingly weak coupling as $\omega$ is increased. The CGHS model (see Sec. II A) corrections are used in the following, i.e., $\epsilon=0$, and so $P(\phi,\epsilon)=1$. The initial value of $\frac{d\phi}{ds}$ is then zero at $\phi_0=\frac{1}{2}\ln 2$, unless $\omega=\frac{1}{2}$.

One can divide the cases first into those for which $\omega>$

[1] The Russo-Susskind-Thorlacius (RST) [2] model has $\epsilon=1,\omega=1$.

[2] $\omega$ is multiplied by $\kappa$ in the logarithm if $\kappa$ has not been scaled out.

$\frac{1}{2}$, $\omega = \frac{1}{2}$, and $\omega < \frac{1}{2}$. Then for the former case one has $\phi_0 < \phi_{cr}$, $\phi_{cr} < \phi_0 < \frac{1}{2}\ln 2$, and $\phi_0 > \frac{1}{2}\ln 2$. When $\omega < \frac{1}{2}$, we have $\phi_0 < \frac{1}{2}\ln 2$, $\frac{1}{2}\ln 2 < \phi_0 < \phi_{cr}$, and $\phi_0 > \phi_{cr}$. For $\omega = \frac{1}{2}$, one simply has sub- and supercritical initial values $\phi_0 < \phi_{cr}$ and $\phi_0 > \phi_{cr}$.

One can also compare with the classical counterparts for which $\kappa = 0$ in the field equations. The critical values of $\phi$ do not exist in the classical case.

By inspection of the field equations (4),(5), the regions from which one would like to consider a value of $\omega$ are

$$\omega < 0, \quad \omega = 0, \quad 0 < \omega < \frac{1}{2}, \quad \omega = \frac{1}{2},$$

$$\frac{1}{2} < \omega < 1, \quad \omega = 1, \quad \omega > 1. \tag{12}$$

Lemos and Sa [7] also show that the global structure differs for the cases $1 < \omega < 2$, $\omega = 2$, and $\omega > 2$. The numerical analysis does not distinguish qualitatively between these cases.

We leave until later a fuller discussion of the case $\omega = \frac{1}{2}$.

## III. SOLUTIONS

Since the corrected solutions are static by the ansatz, and there is in general nonzero radiation density outside the black hole due to the Polyakov term associated with the minimal matter fields, they represent equilibrium scenarios. The ADM mass may be calculated as follows [12].

Let $g_{ab} = \eta_{ab} + h_{ab}$ and $\phi = \Phi_L + \varphi$ be perturbations from flat space $\eta_{ab}$ and from linear dilaton $\Phi_L$, where $h_{ab}$ and $\varphi$ vanish at infinity. The total mass measured by an observer at right infinity is given by

$$M = \int t_{0\mu}\xi^{\mu} dx, \tag{13}$$

where $t_{0j}$ comes from the linearized energy-momentum tensor for the classical theory, $\xi^j$ is a timelike Killing vector, and $x$ is a suitable radial coordinate. For this calculation, one needs the generalized asymptotic expansions of $\rho$ and $\phi$. In the case $\omega = 1$, we have these expressions [5]. Below, we shall note the result for this case, which is representative of the $\omega > 0$ cases. It would seem that $M \to \pm\infty$ except when $\omega = 0$. This is due to the thermodynamics peculiar to two dimensions.

There is by construction a horizon on $s = 0$ in all the cases. For example, in the case $\omega = 1$, when one reproduces the classical black hole of Witten [12], there is a curvature singularity at finite negative $s$, behind the horizon at the origin. One can see how the distance from the origin to the singularity decreases as one goes toward the critical value of dilaton. This corresponds to a smaller black hole, which would appear later in a sequence of static black holes that one might use to represent black hole evolution. However, the sequence can never be complete because of the divergences as one approaches the critical value.

### A. Classical solutions

There will be given a set of plots of the numerical regular-horizon solutions of the model with the various values of the parameter $\omega$ considered in [7] for the classical case which has $\kappa = 0$. For $\kappa = 0$, one can show that there exists a timelike killing vector, and so the most general solution is static [13].

In the classical case, the initial value of the gradient of $\phi$ is given by

$$\phi'(0) = -\frac{1}{2}e^{2\rho_0} \tag{14}$$

and $\rho_0 = 0$ is chosen in each case. This initial value is independent of $\omega$. For the initial gradient of $\rho$,

$$\rho'(0) = -\frac{1}{2}(2\omega - 1)e^{2\rho_0}\ , \tag{15}$$

which clearly depends on $\omega$ and goes through zero at $\omega = \frac{1}{2}$. Let the operator

$$D = \frac{d}{ds} + s\frac{d^2}{ds^2}. \tag{16}$$

The classical equations are

$$D\phi = 2s\phi'^2 - \frac{1}{2}e^{2\rho}, \tag{17}$$

$$D\rho = 2s\omega\phi'^2 - \frac{1}{2}e^{2\rho}(2\omega - 1). \tag{18}$$

Notice that $\phi$ only appears in the equations as a derivative of $s$. This means that it will not matter as far as qualitative changes are concerned what the initial value of $\phi$ is: There are no *critical* values of $\phi_0$. The initial conditions given above are applied, which ensure that the solution is regular at the horizon, $s = 0$. The initial value of $\rho$ simply scales, and is taken in every case to be zero. The coordinates $x^+, x^-$ are analogous to the Kruskal coordinates in the Schwarzschild solution, and cover the extended manifold. The two coordinate invariant functions $\phi$ and the curvature scalar $R$ are plotted, along with the metrical factor $\rho$, for several values of $\omega$.

In order to obtain solutions which are regular at the origin, one has to integrate from the origin in both directions using particular initial conditions on $\rho$ and $\phi$ and their derivatives. The key points are to note singularities or lack of singularities in the curvature and whether they occur at weak or stong coupling in $\phi$, and also to note divergences in $\rho$ and/or $\phi$, while the curvature is finite. Further physical conclusions are difficult to make since these are numerical solutions which are static and thus effectively one-dimensional. The following table gives the legend for the numerical solution plots:

Legend for numerical solutions

| | |
|---|---|
| ---------- | $w = 1.5$ |
| ———— | $w = 1$ |
| -------- | $w = 0.5$ |
| — · — · — · | $w = 0$ |
| — — — — | $w = -1$ |

Our classical numerical results are in agreement with

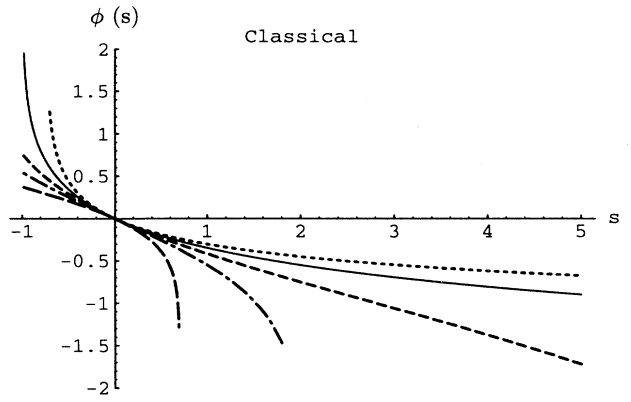


FIG. 1. The dilaton field for the five cases of the $\omega$ parameter at the classical level.

the analytical solutions of [7] for their $A > |B|$, with $\lambda^2 > 0$. It is necessary to reproduce these so that one can compare with the new semiclassical solutions given later. In the following, brief physical comments are made upon each of the solutions, which should be read in conjunction with Figs. 1–3.

### 1. $\omega < 0$

We take for example $\omega = -1$. Towards positive $s$, $\phi$ diverges to minus infinity, while $\rho \to \infty$, at finite coordinate distance. The curvature is approximately constant and negative. Thus we have a timelike right infinity, at weak coupling. To the left we have $\phi \to \infty$, while $\rho \to -\infty$. The curvature goes to $-\infty$, and so we have a timelike singularity. The extended manifold is given in [7], as for all the following classical cases.

### 2. $\omega = 0$

This is the Jackiw-Teitelboim theory considered in [14]. It represents constant curvature anti–de Sitter space with strong coupling to the left and weak coupling to the right. The second field equation above (18) is precisely

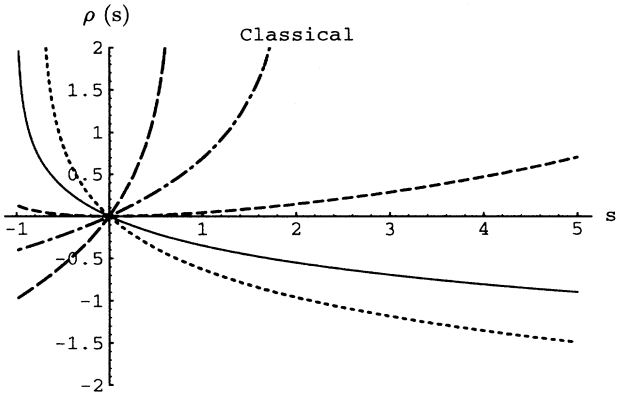


FIG. 2. The conformal factor for the five cases of the $\omega$ parameter at the classical level.

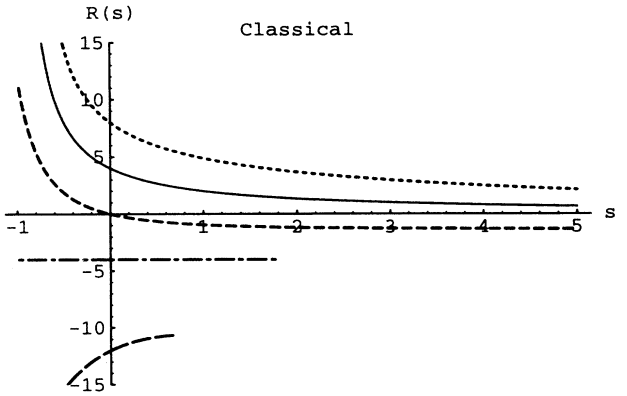


FIG. 3. The scalar curvature at the classical level.

the statement that the curvature scalar will be $R = -4$, and this is borne out in Fig. 3.

### 3. $\omega = \frac{1}{2}$

This is planar general relativity. The gradient of $\rho$ is initially zero. In the above cases it is positive, and becomes increasingly negative as $\omega$ increases. There is a spacelike singularity at strong coupling ($\phi \to \infty$) to the left as in the previous case and for all $\omega > 0$. To the right, $\phi$ diverges to minus infinity, and the curvature tends to a constant negative value. There is thus a black hole with a timelike right infinity.

### 4. $\omega = 1$

This is the classical black hole of Witten [12], which was found in low energy string theory. There is a spacelike singularity at strong coupling ($\phi \to \infty$), and the curvature tends to zero at right infinity, which is null.

### 5. $\omega > 1$

We consider $\omega = \frac{3}{2}$. This has the spacelike singularity at left infinity at strong coupling ($\phi \to \infty$), but at right infinity, $\phi$, $\rho$, and the curvature all go to minus infinity logarithmically. The rate at which the curvature does so increases as $\omega$ increases. This means that these spacetimes have singularities to the right and left, spacelike and timelike, respectively. More details can be found in [7].

## B. Quantum corrections

It is clear that the quantum corrections make significant qualitative changes to the overall structure of the spacetime, as can be seen by comparing the $\phi$, $\rho$, and curvature scalar plots for classical and quantum cases. But one would expect such differences from looking, for example, at the expressions for the curvature scalar as a function of $\omega$, $\phi$, and $\rho$.

The curvature scalar is given by

$$R = -8e^{-2\rho}D\rho. \tag{19}$$

The field equations can be used to rewrite this expression as

$$R_{\rm cl} = 4(2\omega - 1) - 16\omega s\phi'^2 e^{-2\rho}, \tag{20}$$

$$R_q = \frac{4(2\omega - 1) - 16\omega s\phi'^2 e^{-2\rho}}{P(\epsilon,\phi)^2 - \omega e^{2\phi}} \tag{21}$$

in the classical and quantum-corrected cases, respectively. Therefore at weak coupling ($\phi << 0$), the two quantities may be approximately equal, but clearly, there are large effects near the critical value. Indeed, several examples will be seen of the "semiclassical" type of singularity which happens when $\phi$ hits the critical value. Let us define the *semiclassical singularity* to be one where the dilaton field is finite. The coordinates may or may not diverge at this point, but this clearly depends on the coordinate system. The key difference between this singularity and the classical ones is simply that the dilaton field no longer diverges there. Note that if $\omega \leq 0$ there can be no semiclassical singularities, although in some cases there are still qualitative differences in causal structure due to the corrections.

### C. Quantum solutions

In the work of [4], given in their Fig. 2, $\phi_{\rm cr} = -2$, and $\kappa = e^4$. One should note again that this singularity occurs at finite $\phi$ and $\rho$. Indeed, for this choice of $\kappa$, the singularity is actually at weak coupling $g_s = e^{-2}$. The same equations have been solved here in the case $\omega = 1$, with the same initial conditions but different $\kappa$ and initial value of dilaton. The results are qualitatively identical as expected.

In the new plots given here, $\kappa$ and $\lambda$ have been scaled out of the equations by using field redefinitions of the variables $\rho$ and $\phi$. For the quantum case, in general, three sets of graphs for each value of $\omega$ are needed, whereas in all the classical plots, $\phi$ ranges $(-\infty, +\infty)$. In Fig. 4, for $\omega = 1$, however, $\phi < 0$. Witten [12], regarded the dilaton field as a coordinate-independent measure of an observer's position. Viewing it as such, one might believe some of space to have been omitted as the region $\phi \geq 0$ does not exist. This is why we may need to plot more than one graph for each $\omega$. Then, combining the

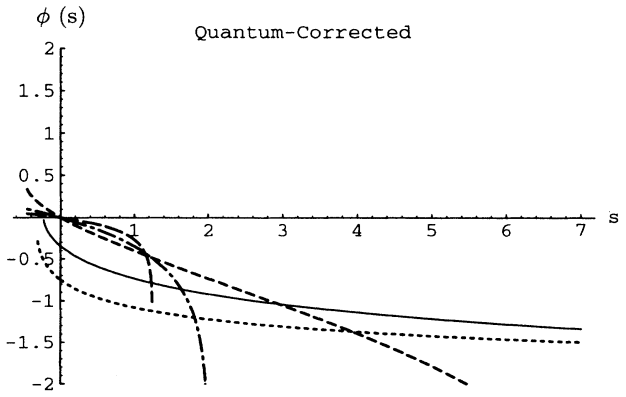


FIG. 4. The dilaton at the semiclassical level for the subcritical initial value.

solutions, $\phi$ ranges $(-\infty, +\infty)$ as in the classical case. Although there will be a singularity as $\phi$ goes through the critical value, the metric will be finite there, unlike at the classical counterparts. It is not sensible, in the context of semiclassical dilaton gravity, to talk about how objects could pass through the singularity. However, one can find solutions for values of $\phi$ above critical, and thus approach the singularity from "either side" as far as the dilaton is concerned.

As one approaches the critical value, however, the equations which are derived here from the action (1) no longer represent the quantum theory of the action. This is because the graviton-dilaton loops become comparable to the large $N$ matter field corrections. Thus, it is not clear how one should interpret the semiclassical singularity. One cannot make definite statements because we do not have a perturbative expansion or exact theory which indicates whether or not it persists. On either side of the singularity, however, the equations should be reliable.

In [4], purely supercritical solutions were considered interesting, and such a solution, that of constant curvature space, was presented. There exist four-dimensional extremal black hole solutions for which the asymptotic dilaton value is supercritical [9]. For this reason, this author believes that it is useful to include the supercritical solutions here, even if some of the section on planar general relativity is superceded, because the quantum theory may turn out not to have a well-defined evolution through the critical value.

The semiclassical appearance of a singularity is a limitation. It cannot be integrated through numerically and there is no contact between the sub- and supercritical dilaton regions of spacetime. A smoothed singularity should be passed through by test particles. In that case it seems plausible that one consider how to paste together semiclassical spacetimes which display singularities which do not appear at infinitely strong dilaton coupling. Naturally, an objection is that one has to reapply boundary conditions for the supercritical region, and so the solutions may have nothing to do with the subcritical ones. However, it is plausible to apply equivalent conditions. This is supported by the fact that the dilaton field is continuous across the critical line when one considers attaching sub- and supercritical solutions.

As long as one has a classical spacetime picture, it would seem difficult to go further than this. However, it is precisely this type of operation that one has in mind for evaporating black holes which develop baby universes. The spacelike boundary is removed and replaced with a region to the future, disconnected from the external space.

The quantum-corrected cases are commented upon individually in the following.

### D. Subcritical solutions

Since the critical value is at $\phi_{\rm cr} = -\frac{1}{2}\ln\omega$, the lowest two cases $\omega = 0, -1$ do not have such a critical value. But since there is a change of initial gradient of $\phi$ when $\phi_0 = \frac{1}{2}\ln 2$, we use this to divide the cases, while the other cases $\omega = \frac{1}{2}, 1, \frac{3}{2}$ are genuinely subcritical in the Figs. 4–

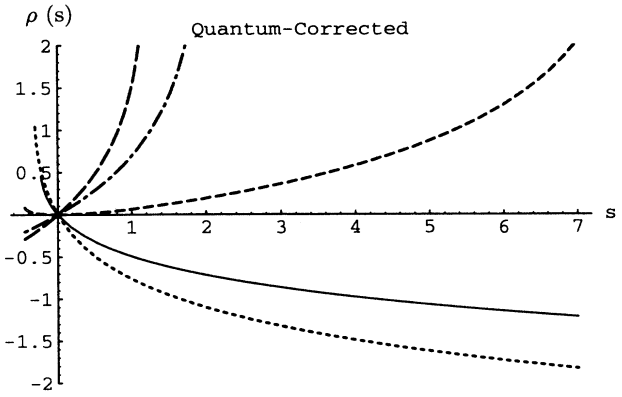


FIG. 5. The conformal factor at the semiclassical level for the subcritical initial value.

6. Generally speaking, the subcritical corrected cases resemble their classical partners at weak coupling, which is why subcritical solutions have received more attention. The differences become clearer as the critical value is approached from below.

### 1. $\omega = -1$, $\phi_0 = 0$

This case covers the qualitative behavior for all $0 > \omega > -\infty$. At strong coupling toward negative $s$, the curvature goes to minus infinity at $s = -\infty$. To the right, $\phi \to -\infty$ and $\rho \to \infty$ at finite $s$, while the curvature is always negative and finite. Thus we have a timelike *classical type* singularity to the left, and timelike infinity to the right, rather like the extremal Reissner-Nordstrom spacetime in four dimensions. This does not differ globally from the classical case.

### 2. $\omega = 0$, $\phi_0 = 0$

The classical and quantum types of singularity coincide, because the place where the quantum singularity occurs in the case of $\omega = 0$ is at infinity, as in the classical case.

This is again anti–de Sitter space. The global structure is the same as for the classical case, though the dilaton goes to infinity toward the left in a logarithmic fashion in the corrected case. Lemos and Sà showed that the classical Jackiw-Teitelboim theory contains a nonsingular black hole, and this would appear to apply also to the quantum-corrected case. This black hole has zero radiation density as $\omega = 0$, and zero temperature, as Cadoni and Mignemi showed [15].

### 3. $\omega = \frac{1}{2}, 1, \frac{3}{2}$

For $\omega = \frac{1}{2}$ the critical value coincides with the important value $\phi = \frac{1}{2}\ln 2$ [see (10)].

Each of these cases has a spacelike singular black hole to the left, as do higher values of $\omega$. The singularities occur at finite $\phi$, and so the $\phi$ (Fig. 6) and $\rho$ (Fig. 7) graphs are truncated behind the horizon. In the asymptotic region to the right, the behavior is classical as expected at weak coupling for subcritical plots, quantum corrections being small; the cases $\omega = \frac{1}{2}$ and $\omega = 1$ are asymptotically anti–de Sitter and flat spaces, respectively, whereas for $\omega > 1$ the curvature goes to minus infinity logarithmically, giving a timelike singularity, though this fact is not clear from Fig. 6, but can easily be confirmed by plotting to larger $s$. This zero coupling timelike singularity seems somewhat unphysical. The $\omega = 1$ case agrees with the work of Birnir *et al.* [4]. From the generalized asymptotic expansion given in [5],

$$\rho = \ln 2b - \frac{K + L\ln s}{s^{2b}} + \left[\frac{K + L\ln s}{s^{2b}}\right]^2 + \cdots, \tag{22}$$

where $K$, $L$, and $b$ are arbitrary constants to be determined, and

$$\phi = \rho - b\ln s - c. \tag{23}$$

Using (13), in terms of the coordinate $2x = b\ln s + 2c$, where $c$ is a constant, the ADM mass is

$$M = e^{2c}\left(K + \frac{1}{2b}L(x+\alpha)\right)_{x\to\infty}, \tag{24}$$

where $\alpha$ is a constant. The mass is therefore formally infinite, as was seen in [4].

It is because of the correspondence with classical the-

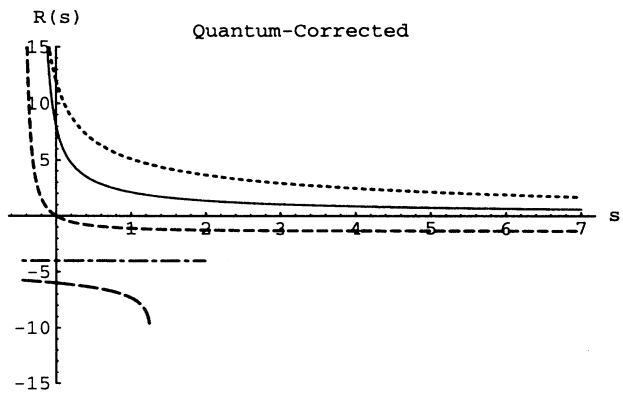


FIG. 6. The curvature at the semiclassical level for the subcritical initial value.

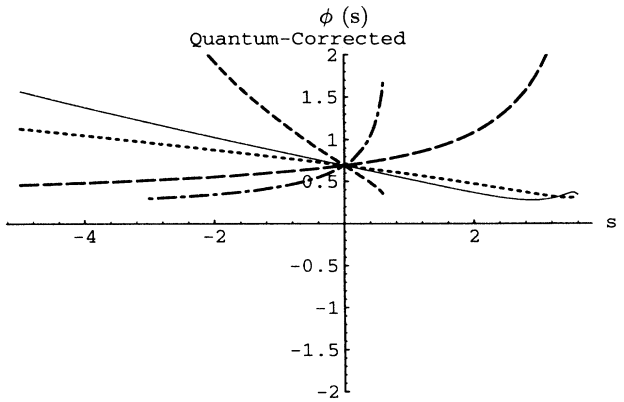


FIG. 7. The dilaton at the semiclassical level for the supercritical initial value.

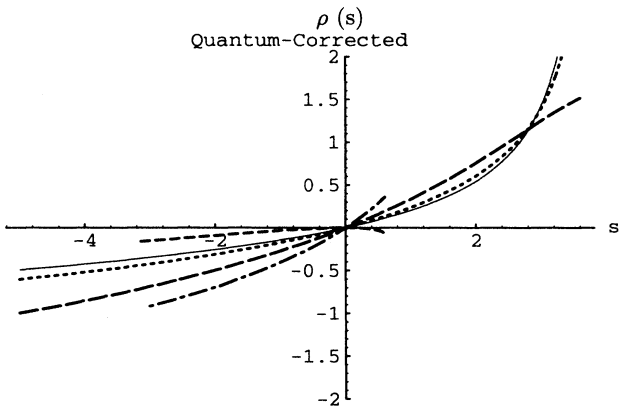


FIG. 8. The conformal factor at the semiclassical level for the supercritical initial value.

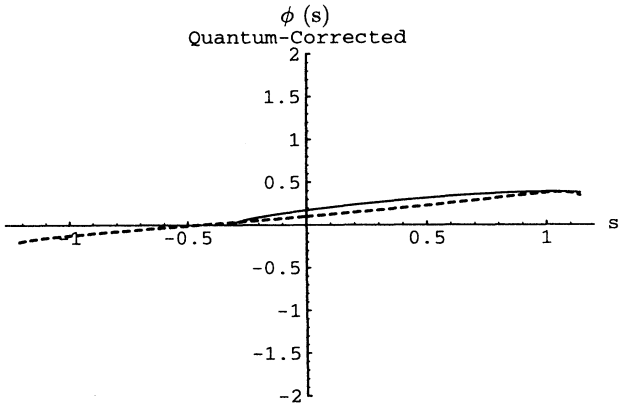


FIG. 10. The dilaton for $\omega = 1, \frac{3}{2}$ at the semiclassical level for the initial value which is above critical but below $\frac{1}{2}\ln 2$.

ory that we regard the subcritical case as physically interesting. But this has meant that the supercritical case has been left uninvestigated and the semiclassical singularity mysterious. In the following "the other side" of the singularity, on which the dilaton is supercritical, and which was originally termed the "Liouville region," is considered.

### E. Supercritical solutions

The supercritical initial value is taken to be $\phi_0 = \ln 2$ in the following five cases, which are given in Figs. 7–9. For the cases $\omega = 1, \frac{3}{2}$, there is another region between the critical value and $\phi_0 = \frac{1}{2}\ln 2$ in which the dilaton remains confined. This additional supercritical pair of solutions is given in Figs. 10–12 for completeness.

#### 1. $\omega = -1, 0$

Now the strong coupling region is toward positive $s$, and $\phi$ decreases slowly at negative $s$. The space is again anti–de Sitter space for $\omega = 0$, while for $\omega = -1$ the curvature varies from zero at positive $s$, to $-4$ at negative $s$, where the spacetime approaches the anti–de Sitter space of the $\omega = 0$ case.

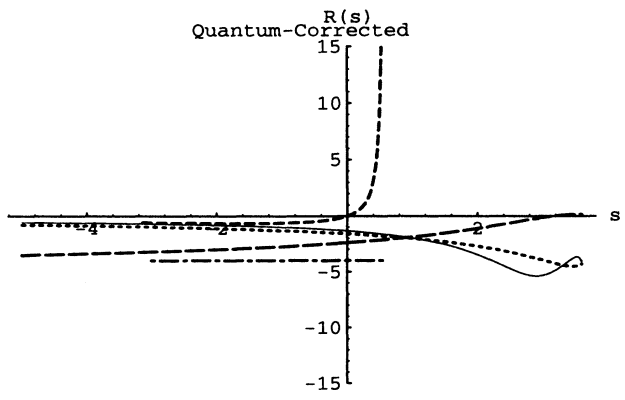


FIG. 9. The curvature at the semiclassical level for the supercritical initial value.

#### 2. $\omega = \frac{1}{2}$

This is the only case which has a spacelike singularity; the other cases are disconnected from their critical values in this region. In particular, the critical value is $\phi_{cr} = \frac{1}{2}\ln 2$. To the left $\phi$ diverges but the curvature is negative and slowly varying, while to the right, there is a singularity hidden by a horizon. We return to this case below.

#### 3. $\omega = 1, \frac{3}{2}$, $\phi_0 > \frac{1}{2}\ln 2$

These have finite curvature everywhere in this region. Toward negative $s$, at strong coupling, the space is asymptotically flat, while toward positive $s$, as $\phi \to \frac{1}{2}\ln 2$, the curvature $R \to -4$. These results are in Figs. 7–9.

#### 4. $\omega = 1, \frac{3}{2}$, $\phi_{cr} < \phi_0 < \frac{1}{2}\ln 2$

One can also consider the region immediately above the singularity as far as $\phi$ is concerned for these param-

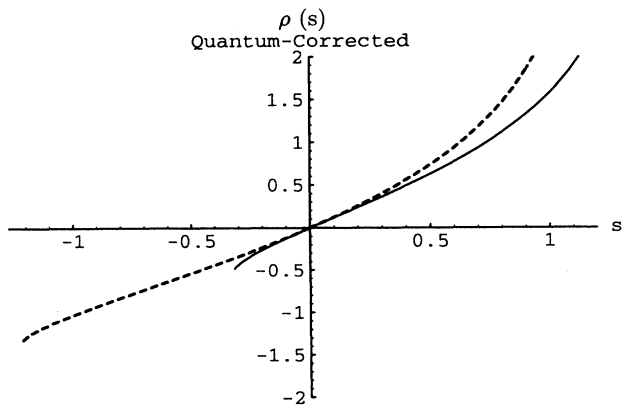


FIG. 11. The conformal factor for $\omega = 1, \frac{3}{2}$ at the semiclassical level for the initial value which is above critical but below $\frac{1}{2}\ln 2$.

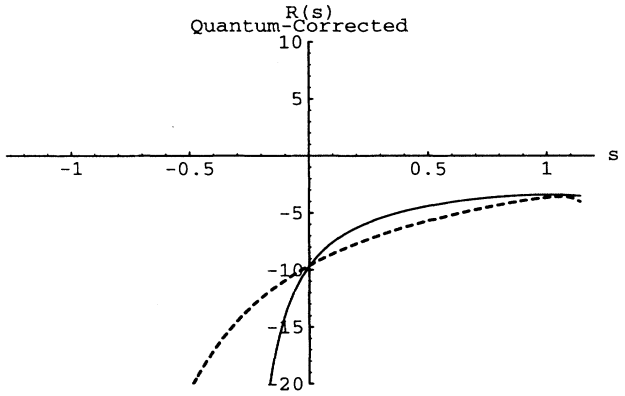


FIG. 12. The curvature for $\omega = 1, \frac{3}{2}$ at the semiclassical level for the initial value which is above critical, but below $\frac{1}{2}\ln 2$.

eter values. The two examples are qualitatively similar. They have a timelike singularity at negative $s$ as the dilaton descends toward the critical value, and have approximately constant negative curvature at positive $s$, where $\phi \to \frac{1}{2}\ln 2$ and $\rho$ diverges. These comments are given graphically in Figs. 10–12.

### F. Planar general relativity

The classical core of this case has been discussed in [16]. The classical solution given earlier is actually a solution of general relativity. In this case, there are only two regions necessary to cover all values of $\phi$ along the real line, because the critical value coincides with the value $\phi = \frac{1}{2}\ln 2$, which was discussed earlier. Generally, in such cases where there exists a finite region $\phi_{\rm cr} < \phi < \frac{1}{2}\ln 2$, there is a solution in which the dilaton is confined between these outside values so that a third initial value will be necessary for the dilaton to range the full real line. Consider the results given in Figs. 4 and 7. The curve $\omega = \frac{1}{2}$ in Fig. 7 increases monotonically from the asymptotic region at the right until it reaches $\phi_{\rm cr} = \frac{1}{2}\ln 2$ when there is a singularity and the integration breaks down. In Fig. 4, the curve descends monotonically to this value and has the same gradient there. If one were to attach these two curves, the dilaton would be a continuous monotonic function *through* the singularity. There would be a small discontinuity in the conformal factor there. For other asymmetric initial dilaton values, the dilaton curve is no longer smooth, but it remains monotonic and piecewise continuous. The reader is reminded, however, that the equations are not valid at the singularity, and so this point may not be important in a fuller theory.

The Penrose diagrams for the extended spacetime corresponds to the two sets of solutions are given in Fig. 13. Dashed regions are copies of their undashed counterparts.

At the spacelike singularities of both boxes, $\phi = \frac{1}{2}\ln 2$. One could draw a line from the timelike infinity in case 1, region I, where $\phi = -\infty$, through the singularity, where one identifies with a point on the lower singularity of case 2, and on through region II′, out to timelike infinity in region I′ where $\phi \to \infty$. A plausible pasting together of the

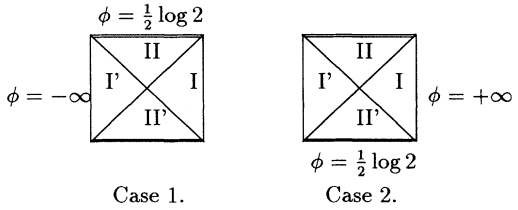


FIG. 13. Penrose diagrams of quantum-corrected planar general relativity.

two spacetimes would be to place the box corresponding to case 2 on top of that of case 1 and identify the singularities where the dilaton is $\frac{1}{2}\ln 2$. This is very literally "toy modeling." The interpretation of the resulting single diagram is open to debate. As expected, there is now a singularity at finite coupling in the *middle* of the diagram. Semiclassically, the singularity is final. However, in quantum gravity, the singularity may be smoothed, and test particles may be able to pass through the region of high curvature. The diagram here suggests a strong curvature wormhole shrouded on either "side" by a horizon, at which the curvature goes through zero, and is asymptotically anti–de Sitter space.

An observer who begins in the asymptotic region I of case I could avoid the wormhole by constantly accelerating immediately to timelike infinity, when $\phi = -\infty$, staying in region I. Alternatively, he might remain stationary, in which case he would pass through the wormhole at $\phi = \frac{1}{2}\ln 2$, after which he could constantly accelerate so that he reached another timelike infinity in the second box, where $\phi = \infty$.

## IV. CONCLUSIONS

A general, two-dimensional model has been considered and solved numerically for static, equilibrium solutions. There are many configurations which depend on both the value of the parameter $\omega$ and on the initial value of the dilaton field at the origin.

The classical solutions found bore out the results of [1] and the semiclassical $\omega = 1, \phi < \phi_{\rm cr}$ case those of [4]. The extreme Reissner-Nordström-type solution $\omega = -1$, the Schwarzschild-type black hole $\omega = 1$, of low energy string theory, the black hole with timelike anti–de Sitter infinity $\omega = \frac{1}{2}$, of planar general relativity, the spacetime with both timelike and spacelike singularities, $\omega = \frac{3}{2}$, and the nonsingular Jackiw-Teitelboim black hole $\omega = 0$ were all seen both classically and at the semiclassical level, where they in general represented black holes in the Hartle-Hawking equilibrium state. These subcritical solutions are the most clearly physically interesting solutions since they correspond with their classical counterparts and four-dimensional analogues. Of all these solutions, the unique parameter value, which yields a solution which has everywhere positive curvature and is asymptotically flat, is that of string theory, $\omega = 1$.

Supercritical solutions for all cases were also found, and for $(\omega = \frac{1}{2})$, it appeared plausible to paste the supercritical to the subcritical solution. Then, as in clas-

sical theories, the dilaton ranges the full real line and is continuous across the singularity. This construction is not possible in classical theory since in that case the singularity always occurs at a divergent dilaton field.

At the semiclassical level, the two regions are still divided by a curvature singularity. This singularity was not expected originally [1], and was met with puzzlement when discovered in subsequent work [8, 9, 4]. In the RST model, the singularity is taken seriously as a "central" boundary, analogous to the origin in Schwarzschild spacetime. However, it is known that there are energy conservational problems at the end point [17], which may be related to this potential misinterpretation. The equations which generate the singularity become inappropriate in its vicinity, but one can still consider subcritical and supercritical solutions independently.

The singularity is a modification to classical theory which may or may not go away in quantum gravity or is generically spurious. Birnir *et al.* [4] discussed the possibility of sailing through this mild singularity. Horowitz and Marolf [18] have recently discussed the behavior of quantum test particles which have well-defined motion even in singular spacetimes.

## ACKNOWLEDGMENTS

I thank Stephen Hawking and Gary Gibbons for reading the paper, and for conversations and suggestions.

[1] C.G. Callan, S.B. Giddings, J.A. Harvey, and A. Strominger, Phys. Rev. D **45**, R1005 (1992).

[2] J.G. Russo, L. Susskind, and L. Thorlacius, Phys. Rev. D **46**, 3444 (1992); **47**, 533 (1993).

[3] J.A. Harvey and A. Strominger, in *Recent Directions in Particle Theory: From Superstrings and Black Holes to the Standard Model*, Proceedings of the Theoretical Advanced Study Institute, TASI in Particle Physics, Boulder, Colorado, 1992, edited by J. Harvey and J. Polchinski (World Scientific, Singapore, 1993); S.B. Giddings, in *String Quantum Gravity and Physics at the Planck Scale*, Proceedings of the International Workshop of Theoretical Physics, 6th Session, Erice, Italy, 1992, edited by N. Sanchez (World Scientific, Singapore, 1993); A. Strominger, presented at the Les Houches Workshop on Black Holes, Les Houches, France, 1994; T. Banks, "Lectures on Black Holes and Information Loss," Report No. RU-94-91 (unpublished); S.B. Giddings, in *1994 Summer School in High Energy Physics and Cosmology*, Proceedings, Trieste, Italy (World Scientific, Singapore, 1995).

[4] B. Birnir, S.B. Giddings, J.A. Harvey, and A. Strominger, Phys. Rev. D **46**, 638 (1992).

[5] S.W. Hawking, Phys. Rev. Lett. **69**, 406 (1992).

[6] A. Polyakov, Phys. Lett. **103B**, 207 (1981).

[7] J.P.S. Lemos and P.M. Sà, Phys. Rev. D **49**, 2897 (1994); Class. Quantum Grav. **11**, L11 (1994).

[8] J.G. Russo, L. Susskind, and L. Thorlacius, Phys. Lett. B **292**, 13 (1992).

[9] T. Banks, A. Dabholkar, M. Douglas, and M. O'Loughlin, Phys. Rev. D **45**, 3607 (1992).

[10] A. Bilal and C. Callan, Nucl. Phys. **B394**, 73 (1993).

[11] J.D. Hayward, Phys. Rev. D **52**, 1019 (1995).

[12] E. Witten, Phys. Rev. D **44**, 314 (1991).

[13] G.W. Gibbons and M.J. Perry, Int. J. Mod. Phys. D **1**, 335 (1992).

[14] C. Teitelboim, Phys. Lett. **126B**, 41 (1983); R. Jackiw, Nucl. Phys. **B252**, 343 (1985).

[15] M. Cadoni and S. Mignemi, Nucl. Phys. **B427**, 669 (1994).

[16] J.P.S. Lemos, "Two-dimensional Black Holes and General Relativity," Instituto Superior Tecnico Report No. DF/IST-13-93, 1993 (unpublished).

[17] J. Polchinski and A. Strominger, Phys. Rev. D **50**, 7403 (1994).

[18] G. Horowitz and D. Marolf, Phys. Rev. D **52**, 5670 (1995).